Luminescence and energy transfer processes of Sm^{3+} in $K_5Li_2LaF_{10}:Sm^{3+}$-$K_5Li_2SmF_{10}$ single crystals

P. Solarz* and W. Ryba-Romanowski
Institute of Low Temperature and Structure Research, Polish Academy of Sciences, ulica Okólna 2, PL-50422 Wrocław, Poland
(Received 3 March 2005; published 1 August 2005)

Stark sublevels of multiplets of the $4f^5$ electronic shell ion have been determined and the Judd-Ofelt intensity parameters have been calculated. Decay curves of the luminescence originating with the $^4G_{5/2}$ multiplet in $K_5Li_2La_{1-x}Sm_xF_{10}$ ($x=0.01,0.05,0.1,0.25,0.5,1$) crystals have been measured as a function of Sm^{3+} concentration and temperature. A nonexponential character was observed for $x=0.05,0.1,0.25$ at room temperature and also for $x=0.5$ at temperatures below 190 *K*. The generalized Yokota-Tanimoto model has been used to explain the behavior of the decay curves and to determine the kinetic microparameters C_{DA}, related to the cross relaxation, and *D*, related to the energy migration probabilities. The ion-ion interaction has been determined to be strong. The lifetime values of the $^4G_{5/2}$ excited state are close to 7600 μs for $x=0.01$ and 80 μs for $x=1$, independent of temperature.

DOI: 10.1103/PhysRevB.72.075105 PACS number(s): 78.55.−m, 31.70.Hq, 42.70.−a, 76.30.Kg

I. INTRODUCTION

Single crystals of $K_5Li_2SmF_{10}$ have been grown and examined in systematic investigations of the series of compounds $K_5Li_2LnF_{10}$ ($Ln=Pr^{3+},Nd^{3+},Sm^{3+},Eu^{3+}$) to explain the phenomenon of weak-concentration self-quenching of luminescence of Ln^{3+} ions in these crystals. The compounds are found to be uncommon in spectroscopic properties[1–4] because they show exceedingly low luminescence quenching depending on the concentration of active ions. Even fully concentrated crystals, with the ions mentioned above, show efficient luminescence. This type of crystal is a so-called stoichiometric luminescence material or self-activated compound.[5,6] Based on experimental data gathered during recent decades generalizations that help in the assessment of radiative and nonradiative transition rates were made. In particular, the radiative transition rates are mainly evaluated within the Judd-Ofelt theory, where three phenomenological parameters are used. The multiphonon relaxation rates may be predicted based on two parameters derived from the so-called energy gap law. Determination of rates of nonradiative decay due to activator-activator interaction is less straightforward. The parameters needed to characterize migration of the excitation energy and donor-acceptor energy transfer may be derived from analysis of luminescence decay curves and their deviations from a pure exponential time dependence, which are attributed to ion-ion interaction. For qualitative assessment it is assumed that the smallest possible distance between interacting ions is the factor that governs the rate of nonradiative energy transfer. This assumption has been corroborated by results of investigation of oxides like $MNdP_4O_{12}$ ($M=Li,Na,K$), NdP_5O_{14}, $NdAl_3(BO_3)_4$, $Na_5Nd(WO_4)_4$, and $K_5Nd(MoO_4)_4$,[5–9] in which self-quenching of neodymium luminescence has been found to be exceptionally weak. The same trend of weak self-quenching of luminescence has been found in $K_5Li_2EuF_{10}$,[3] where the emission decay curves follow a purely exponential time dependence.

The process of miniaturization in lasers and luminescence materials forces us to find additional stoichiometric luminescence materials because they can allow reduction of the dimensions of solid-state lasers, using diode pumping. What is more, the cooling of small parts is much more effective. We believe that our experimental data help in finding luminescence materials and generalizations of luminescence properties in the lanthanide group, where the luminescence is quenched in two ways. The first one is based on multiphonon relaxation given by the energy gap law. The second one depends on nonradiative energy transfer processes between active ions.

The anomalous, strong electron-phonon coupling in $K_5Li_2SmF_{10}$ has been studied in detail.[10] It breaks the known rule that the strength of the coupling reaches a maximum for trivalent lanthanides from the beginning and the end of these elements, and it is weak in the middle. As a probe of the coupling strength, the Ellens *et al.*[11–13] formula has been used for analysis of the temperature broadening of lines.

In this work an optical analysis of these crystals is described, which includes Judd-Ofelt theory,[14,15] activator-activator interaction,[16–18] and concentration quenching mechanisms of luminescence originating with the $^4G_{5/2}$ multiplet.

II. EXPERIMENT

Single crystals of $K_5Li_2LaF_{10}$ (KLLF) containing the Sm^{3+} ion were grown by the vertical Bridgman method in graphite crucibles made from high-quality IG-110 purified graphite. In this manner, single crystals of $K_5Li_2La_{1-x}Sm_xF_{10}$ (where $x=0.01,0.03,0.1,0.25,0.50,1.00$) have been prepared. All crystals were colorless and transparent with the exception of $K_5Li_2SmF_{10}$ and $K_5Li_2La_{0.5}Sm_{0.5}F_{10}$, which were slightly yellow. The crystals obtained were about 30–50 mm long and 5 mm in diameter.

Luminescence spectra have been recorded upon excitation of the Sm^{3+} ions in these crystals by an argon ion laser (0.45 *W* at wavelength 488 nm, 20 491.8 cm^{-1}). The luminescence was dispersed by a 1 m double-grating monochromator, detected by a Hamamatsu R-928 photomultiplier, av-

TABLE I. Elementary crystal cell parameters of $K_5Li_2LnF_{10}$ stoichiometric crystals.

Lanthanide ion	a (Å)	b (Å)	c (Å)	$a\times b\times c$ (Å^3)	Reference
La	20.775	7.822	6.963	1131.502	2, 19
Ce	20.736	7.805	6.953	1125.305	
Pr	20.733	7.796	6.929	1119.965	
Nd	20.650	7.779	6.902	1108.712	20
Sm	20.628	7.756	6.887	1101.856	
Eu	20.599	7.752	6.879	1098.462	
Gd	20.509	7.709	6.851	1083.170	

eraged by the Stanford model SRS 250 boxcar integrator, and stored in a PC computer. In luminescence decay time measurements, short (4 ns) pulses delivered by an optical parametric oscillator (Continuum, Surelite I) pumped by the third harmonic of a neodymium-doped yttrium aluminum garnet (Nd:YAG) laser were used to excite luminescence levels directly. The decay signal was detected, averaged, and stored with the Tektronix TDS 3052 digital oscilloscope; all decay data were composed of 10 000 points. The fits of experimental decay curves were done using the Microcal ORIGIN V.5.0 software; the amplitude of the curves was calibrated to ten. For absorption measurements the Cary 5E UV-VIS-NIR spectrophotometer was used. For low-temperature measurements a continuous-flow helium cryostat (Oxford model CF 1204) equipped with a temperature controller was used.

III. RESULTS AND DICUSSION

A. Crystal structure

The crystal structure of KLLF was already investigated[2,19,20] but the data were not completed for all La–Gd lanthanide ions. Here we present information on the crystal cell parameters for all lanthanides belonging to the so-called cerium group. The crystals are orthorhombic (space group D_{2h}^{16}, *Pnma*), for all mentioned lanthanide ions, with cell parameters $a\approx 20.7$ Å, $b\approx 7.8$ Å, $c\approx 6.9$ Å (for details see Table I). The crystal structure is built from layers perpendicular to the a axis, formed by LnF_8 dodecahedra and LiF_4 tetrahedra. Lanthanide and lithium ions occupy sites with point C_s symmetry whereas potassium and fluorine ions occupy sites with C_s and C_1 symmetry. The LnF_8 polyhedra do not share fluorine ions and the closest lanthanide ions are separated by about 6.5 Å. Owing to these features, exchange interactions between Ln ions may be neglected. Based on the crystallographic structure, there is only one site for the lanthanide ions.

B. Spectroscopic properties

1. Intensity of transitions

The absorption spectrum of the $K_5Li_2SmF_{10}$ single crystal recorded at room temperature is presented in Fig. 1. It is composed of intense transitions situated in the near infrared ^6F_J ($J=1/2-11/12$) and in the blue-uv ($^6H_{5/2}\rightarrow {}^6P_J$) regions. The intensity of transitions from $^6H_{5/2}$ to $^4G_{5/2}$ is very weak (oscillator strength 2.90×10^{8}). In all the researched $K_5Li_2LnF_{10}$ crystals the hypersensitive transitions are weak;[3,21] to present this fact an inset was placed into Fig. 1 and presents the hypersensitive transition $^6H_{5/2}\rightarrow {}^6F_{1/2}$ marked with an arrow. This fact is unusual. Transitions in which $\Delta J=2$ are known as hypersensitive since their intensities may change even by a factor of 100, from host to host. Hypersensitivity has been intensively studied in the past. To account for experimental data numerous models and hypotheses have been proposed, among others models of inhomogeneous dielectric,[22] covalency,[23] or dynamic coupling.[24,25] None of them is able to explain the experimental data without exceptions, but they lead to the conclusion that the higher the site symmetry, the lower the intensity of the hypersensitive transitions. In this view our finding is puzzling. According to the crystal structure the Sm^{3+} reside in sites of C_s symmetry. The absorption spectrum has been recorded with a good-quality, single-crystal sample. Moreover, measurements were performed with the $K_5Li_2SmF_{10}$ stoichiometric compound to exclude any ambiguity with respect to the Sm^{3+} location, likely to occur when doped crystals are considered.

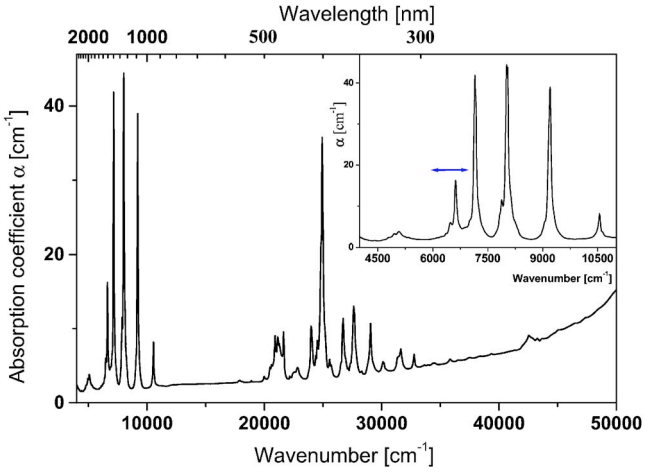

FIG. 1. (Color online) Room-temperature absorption spectrum of $K_5Li_2SmF_{10}$ crystal.

Based on the absorption spectrum the measured oscillator strength values for $f\rightarrow f$ transitions were appointed and presented in Table II. In the frame of Judd-Ofelt[14,15] theory the calculated oscillator strengths are also presented in this table.

The measured oscillator strength of the absorption band is determined experimentally using the following formula:

$$f_{\text{expt}} = 4.138\times 10^{-9}\int \varepsilon(\nu)d\nu \qquad (1)$$

where ε is the molar extinction coefficient at energy ν (cm^{-1}). It should be equal to the electric-dipole and magnetic-dipole oscillator strengths for this transition band, f_{ED} and f_{MD}, respectively. Therefore, we can write

TABLE II. Calculated and measured oscillator strength of $4f^5$ transitions of Sm^{3+} in the $K_5Li_2SmF_{10}$ crystal. $\Omega_2=4.30\times10^{-22}$ cm^2, $\Omega_4=3.60\times10^{-20}$ cm^2, and $\Omega_6=1.84\times10^{-20}$ cm^2.

	Spectral region		Oscillator strength ($\times10^8$)	
Transitions	Wave number (cm^{-1})	Wavelength (nm)	Measured	Calculated
$^6H_{5/2}\rightarrow{}^6F_{1/2-5/2}$, $H_{15/2}$	6717	1488.87	233.62	233.53
$^6H_{5/2}\rightarrow{}^6F_{7/2}$	8143	1228.05	227.10	239.82
$^6H_{5/2}\rightarrow{}^6F_{9/2}$	9287	1076.77	166.01	146.85
$^6H_{5/2}\rightarrow{}^6F_{11/2}$	10556	947.37	25.60	23.19
$^6H_{5/2}\rightarrow{}^4G_{5/2}$	17902	558.61	2.90	ED=0.36 MD=1.85
$^6H_{5/2}\rightarrow{}^6P_{5/2}$, $^4G_{11/2}$	24825	402.83	418.87	391.67
$^6H_{5/2}\rightarrow$ $^6D_{1/2}$, $^4H_{7/2}$	27349	365.64	181.92	198.01
$^6H_{5/2}\rightarrow{}^4K_{15/2}$, $^4H_{11/2}$	29114	343.48	55.46	62.72

$$f_{\text{expt}}=f_{\text{ED}}+f_{\text{MD}} \tag{2}$$

where

$$f_{\text{ED}}=\frac{8\pi mc\nu}{3he^2(2J+1)}\frac{(n^2+2)^2}{9n}S_{\text{ED}},$$

$$f_{\text{MD}}=\frac{8\pi mc\nu}{3he^2(2J+1)}nS_{\text{MD}}, \tag{3}$$

in which formulas the dipole line strengths S_{ED} and S_{MD} are expressed as

$$S_{\text{ED}}=e^2\Omega_t|\langle f^N[L,S]J||U^{(t)}||f^N[L',S']J'\rangle|^2,$$

$$S_{\text{MD}}=\frac{e^2h^2}{16\pi^2m^2c^2}|\langle f^N[L,S]J||\hat{L}+2\hat{S}||f^N[L',S']J'\rangle|^2. \tag{4}$$

In above formulas (3) and (4), n is the refractive index of the medium ($n=1.40$ was used in calculations),[26] J denotes the total angular momentum of the starting state, c means the speed of light in vacuum, m signifies the mass of an electron, and e represents the electric charge of an electron. $\langle f^N[L,S]J|$ and $|f^N[L',S']J'\rangle$ express the wave function of the states taking part in the transition. $\hat{L}+2\hat{S}$ represents the magnetic-dipole operator while $U^{(t)}$ are the matrix elements of the doubly reduced unit tensor.

The radiative transition possibility A is given by the sum of electric-dipole A_{ED} and magnetic-dipole A_{MD} transition probabilities where

$$A_{\text{ED}}=\frac{64\pi^4\nu^3}{3h(2J+1)}\frac{n(n^2+2)^2}{9}S_{\text{ED}},$$

$$A_{\text{MD}}=\frac{64\pi^4\nu^3}{3h(2J+1)}n^3S_{\text{MD}}. \tag{5}$$

Knowing the radiative transition rate (A) between two states, the total radiative transition rate (A_r) can be given as $A_r=\Sigma A$, which gives the possibility to calculate the radiative lifetime (τ_r):

$$\tau_r=A_r^{-1}. \tag{6}$$

A measure of the quality of the fitting is the rms deviation (ΔP) between measured and calculated oscillator strengths, determined by the relation

$$\Delta P=\sqrt{\frac{\sum(\Delta f)^2}{X-Y}} \tag{7}$$

where X is the number of analyzed bands and Y is the number of fitted parameters.

The error in numeric calculation of the Judd-Ofelt intensity $\Omega_{2,4,6}$ parameters is equal to 6.6% and mainly depends on the Ω_2 uncertainty. For the calculated $^6H_{5/2}\rightarrow{}^4G_{5/2}$ transition the magnetic-dipole transition is over five times stronger then the electric-dipole one (see Table II).

Using the calculated $\Omega_{2,4,6}$ intensity parameters, the branching ratio of the transition from the $^4G_{5/2}$ multiplet and the lifetime of this level were calculated. The data for the branching ratio are placed in Table III. The reduced matrix elements $U^{(2)}$, $U^{(4)}$, and $U^{(6)}$ placed in the table were taken from Jayasankar and Rukmini.[27] Nearby half of the luminescence intensity from the $^4G_{5/2}$ multiplet is emitted in the $^4G_{5/2}\rightarrow{}^6H_{7/2}$ transition. Other efficient transitions are $^4G_{5/2}\rightarrow{}^6H_{5/2}$ (15%), $^4G_{5/2}\rightarrow{}^6H_{9/2}$ (20%), and $^4G_{5/2}\rightarrow{}^6H_{11/2}$ (13%), which make the material a red-emitting phosphor. These results agree with observed luminescence spectra (recorded at 4.2 and 300 K) shown in Fig. 2.

Looking at Fig. 2, one can see the strong electron-phonon coupling manifested in the temperature broadening of the samarium emission lines at room temperature. This fact was the point of detailed investigations reported in our previous work.[10] Duffy *et al.* observed also such line broadening in crystals but did not comment on it.[28] It seems that the Sm^{3+} has the strongest electron-phonon coupling, although it is neither at the beginning nor the end of the lanthanide series.

TABLE III. Branching ratios (β) of radiative transitions starting in the $^4G_{5/2}$ level of Sm^{3+} in the $K_5Li_2SmF_{10}$ crystal. $U^{(2)}$, $U^{(4)}$, and $U^{(6)}$ after Ref. 21.

$^4G_{5/2}\rightarrow$	Lower-state energy (cm^{-1})	Transition energy (cm^{-1})	Wavelength of transition (nm)	$U^{(2)}$	$U^{(4)}$	$U^{(6)}$	A_r (s^{-1})	β (%)
$^6H_{5/2}$	0	17724	564.21	0.0003	0.0006	0.0000	ED=3.60 MD=18.49	15.35
$^6H_{7/2}$	1077	16647	600.71	0.0001	0.0086	0.0089	65.27	45.36
$^6H_{9/2}$	2328	15396	649.52	0.0112	0.0067	0.0020	30.63	21.29
$^6H_{11/2}$	3699	14025	713.01	0.0000	0.0053	0.0021	18.89	13.13
$^6H_{13/2}$	5146	12578	795.04	0.0000	0.0002	0.0018	2.41	1.67
$^6F_{1/2}$	6490	11234	890.15	0.0010	0.0000	0.0000	0.01	0.01
$^6H_{15/2}$	6633	11091	901.63	0.0000	0.0000	0.0002	0.15	0.10
$^6F_{3/2}$	6736	10988	910.08	0.0011	0.0001	0.0000	0.16	0.11
$^6F_{5/2}$	7243	10481	954.11	0.0072	0.0017	0.0000	2.17	1.51
$^6F_{7/2}$	8143	9581	1043.73	0.0000	0.0017	0.0002	1.70	1.18
$^6F_{9/2}$	9287	8437	1185.26	0.0018	0.0003	0.0002	0.27	0.19
$^6F_{11/2}$	10556	7169	1394.99	0.0000	0.0001	0.0005	0.14	0.10

This implies that the thesis of Ellens *et al.*[11–13] about the strength of electron-phonon coupling should be reconsidered, especially as the investigated crystal matrix (in Refs. 11–13 and 20) was the same—$LiYF_4$. Understanding of this fact is not clear at the moment, because the Ω_2 intensity parameter in the pseudoquadrupole vibronic transition responds also to the strength of electron-phonon coupling in agreement with the dynamic coupling model.[29] In $K_5Li_2SmF_{10}$ the Ω_2 intensity parameter is extremely small in agreement with the very low intensity of hypersensitive transitions.[3]

2. Dynamics of excited state and self-quenching of luminescence

The measured lifetimes of the $^4G_{5/2}$ state, for the analyzed concentrations, are $x=0.1$, 7618 μs; $x=0.05$, 4900 μs; $x=0.1$, 2523 μs; $x=0.25$, 445 μs; $x=0.5$, 296 μs, and $x=1$, 79μs. The radiative lifetime (τ_r) of the $^4G_{5/2}$ multiplet is 6949.58 μs. A little disagreement between the calculated and measured lifetimes, for strongly diluted crystals with samarium, can be explained by the reduction of distance between Ln ions for La and Sm ions in this matrix (see Table I). The lifetimes presented here are bigger than those met in the literature, even in comparison with other fluorides ($LiYF_4:Sm^{3+}$, 4.0 ms, $KY_3F_{10}:Sm^{3+}$, 4.9 ms),[30] or oxyfluoroborate[31] and fluoroborate glasses,[32] 0.34 and 3 ms, respectively.

Figure 3 presents the rate of nonradiative ion-ion transitions ($W_{i\text{-}i}$) as a function of Sm^{3+} ion concentration. The measured transition rate (A_m) can be assumed as the sum of radiative (A_r), ($W_{i\text{-}i}$), and multiphonon transitions (A_{MP}). That is why we can obtain the rate of ion-ion transitions as

$$W_{i\text{-}i} = A_m - (A_r + A_{MP}). \quad (8)$$

A_r and A_{MP} should not be dependent on the active ion concentration although we should remember about the small lan-

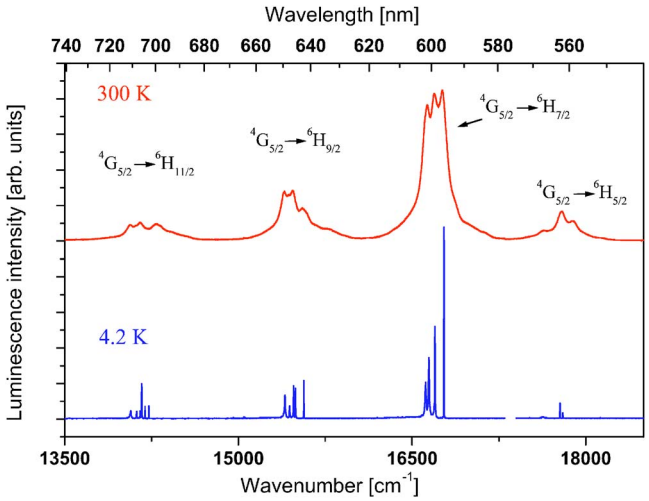

FIG. 2. (Color online) Emission spectra of $K_5Li_2SmF_{10}$ crystal recorded at 4.2 K and room temperature.

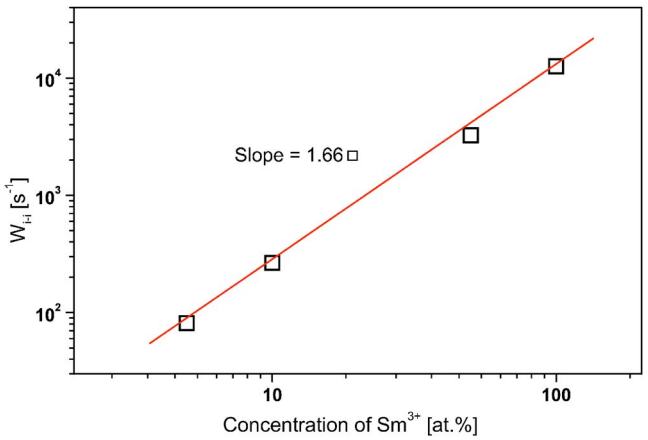

FIG. 3. (Color online) Influence of Sm^{3+} concentration on self-quenching rate of the $^4G_{5/2}$ level.

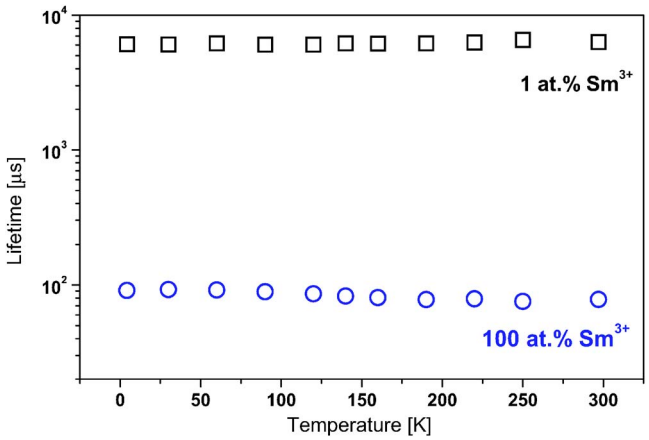

FIG. 4. (Color online) Influence of temperature on the lifetime of the $^4G_{5/2}$ level in $K_5Li_2La_{0.99}Sm_{0.01}F_{10}$ and $K_5Li_2SmF_{10}$ crystals.

thanide contraction. In the investigated material the lifetime for diluted Sm crystals is about the same as radiative one (A_r), so it can be supposed that A_{MP} is equal to zero. This makes it possible to put down the formula for $W_{i\text{-}i}$ as a function of concentration C in at. %:

$$W_{i\text{-}i} = aC^n, \tag{9}$$

where n describes the power of self-quenching processes and a represents a constant. This formula can be simply converted to

$$\log_{10}(W_{i\text{-}i}) = \log_{10}(a) + n\log_{10}(C) \tag{10}$$

The slope n of about unity corresponds to small ion-ion interactions, whereas $n \approx 2$ describes the phenomenon of strong quenching via ion-ion interactions. The experimentally derived slope $n=1.66$, presented in Fig. 3, means that the concentration quenching may be considered strong.

The literature on neodymium-doped crystals contains reports on systems in which a strong self-quenching changes to weak self-quenching with increase of the activator content.[33] However, no such transition has been observed in this $K_5Li_2LaF_{10}:Sm^{3+}$ system. Similar behavior was observed in $K_5Li_2LaF_{10}$ doped with Eu^{3+} for analyzing the self-quenching of the $^5D_1$, $^5D_2$, and $^5D_3$ levels.[3]

Figure 4 presents the influence of temperature on the lifetime of the $^4G_{5/2}$ multiplet in $K_5Li_2SmF_{10}$ and $K_5Li_2La_{0.99}Sm_{0.01}F_{10}$ crystals. Other concentrations were omitted for clarity of the picture. It can be seen that there is no change of lifetime for all concentrations presented as a function of temperature–the lifetime is stable for all amounts of admixture. This can be explained based on the data in Table IV, which presents the low-temperature structure of Stark sublevels of Sm^{3+} multiplets of the $^6H_{5/2}$ to $^4G_{7/2}$ transition in the crystal. The energetic structure of higher-lying multiplets was not assigned because of their rich and superimposed structure. Also the $^6H_{13/2}$ position is lacking, because the transitions to this level were not observed in absorption and emission spectra.

It can be seen that there are possibilities of cross-relaxation processes:

$$^4G_{5/2} \rightarrow {}^6F_{11/2} = {}^6H_{5/2} \rightarrow {}^6F_{5/2},$$

$$^4G_{5/2} \rightarrow {}^6F_{5/2} = {}^6H_{5/2} \rightarrow {}^2F_{11/2}.$$

Such processes are in resonance (within the spectral line half-width at 4.2 K) which makes them temperature independent as shown in Fig. 4.

The decay curves of luminescence for all analyzed concentrations of Sm^{3+} recorded upon direct excitation of $^4G_{5/2}$ at room temperature are presented in Fig. 5. For the concentration of 1 at. % of Sm^{3+} the decay curve is purely exponential. The nonexponential character of the decay curve begins at 5 at. % of Sm^{3+} in the crystal and is well observed for 10

TABLE IV. The Stark sublevel of $4f^5$ Sm^{3+} in $K_5Li_2SmF_{10}$ at 4.2 K.

Multiplet of Sm^{3+}	Stark sublevels expected (observed)	Energy (cm^{-1})	ΔE
$^6H_{5/2}$	3 (3)	0, 25, 166	166
$^6H_{7/2}$	4 (4)	1032, 1110, 1163, 1191	159
$^6H_{9/2}$	5 (5)	2242, 2315, 2332, 2366, 2406	164
$^6H_{11/2}$	6 (6)	3581, 3614, 3643, 3658, 3687, 3739	158
$^6H_{13/2}$	7 (0)		[a]
$^6F_{1/2}$	1 (1)	6376	0
$^6F_{3/2}$, $^6H_{15/2}$	10 (2)	6621, 6633	22[a]
$^6F_{5/2}$	3 (3)	7143, 7150, 7177	34
$^6F_{7/2}$	4 (4)	7978, 8006, 8041, 8050	72
$^6F_{9/2}$	5 (3)	9159, 9200, 9226	67
$^6F_{11/2}$	6 (6)	10517, 10543, 10559, 10583, 10595, 10644	127
$^4G_{5/2}$	3 (3)	17650, 17791, 17816	166
$^4F_{3/2}$	2 (0)		[a]
$^4G_{7/2}$	4 (4)	19982, 20044, 20122, 20150	168

[a]Sublevels to be found.

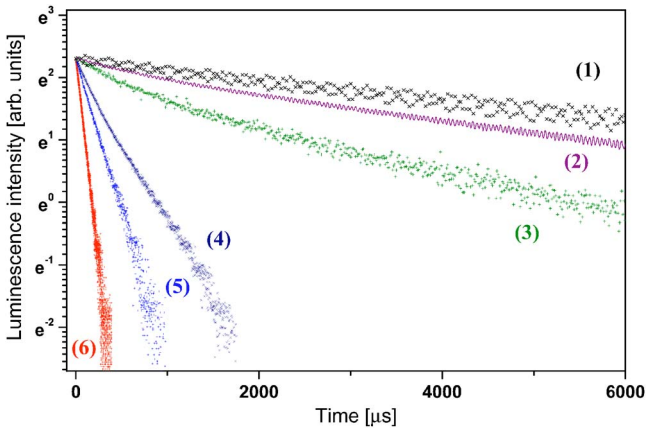

FIG. 5. (Color online) Decay curves of luminescence for analyzed concentrations of samarium, recorded at room temperature. (1) 1, (2) 5, (3) 10, (4) 25, (5) 50, and (6) 100 at. % of Sm^{3+}.

and 25 at. % of Sm^{3+}. The decay curves of luminescence of more concentrated crystals (50 and 100 at. % of Sm^{3+}) become purely exponential again.

The change of the character of the decay curve from exponential to nonexponential and then to exponential anew, with the increase of activator concentration, suggests that for low concentration the interactions between ions are too small to change the shape of the decay curve. For higher concentration the multipolar interaction can change the decay curve to nonexponential. In the case of the highest concentration, fast migration of energy manifests in the material and the curve appears exponential again. The migration of energy should be dependent on the temperature. Figure 6 presents this effect for crystals containing 25 and 50 at. % of Sm^{3+}. At 4.2 K both curves for 25 and 50 at. % of Sm^{3+} are not exponential; at 190 K the curve representing the decay of luminescence becomes an exponential one. Rather the same process appears with the curves describing the decay for 25 at. % of Sm^{3+}, but the migration processes are weaker in this case and it can be seen that the curve is not exponential even at room temperature.

Nonexponential decay curves give the possibility to determine the nature of the ion-ion interaction [dipole-dipole

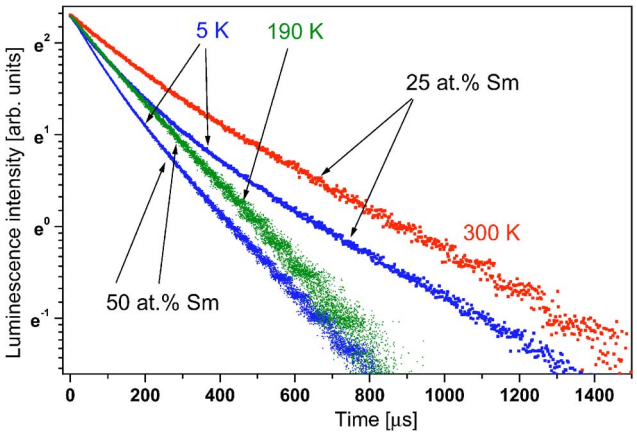

FIG. 6. (Color online) Influence of temperature in changing the character of decay curves from nonexponential to exponential.

(DD), dipole-quadrupole (DQ), or quadrupole-quadrupole (QQ)]. To determine this the generalized model of Inokuti and Hirayama was used.[16] In this model the experimental decay curve can be described as

$$I(t) = (\text{offset}) + I(0)\exp\left(-\frac{t}{\tau_r} - C_A Q t^{3/S}\right) \tag{11}$$

were Q is the energy transfer parameter, offset describes the y-axis shift of the experimental curve, and S signifies the multipolar mechanism and is 6 for DD, 8 for DQ, and 10 for QQ electrostatic interaction. The C_A parameter represents the concentration of active ions, in this case Sm^{3+} ions. Q is described by the formula

$$Q = \frac{4\pi}{3}\Gamma\left(1 - \frac{3}{S}\right)(C_{DA}^{(S)})^{3/S}. \tag{12}$$

Formula (10) describes the quenching mechanism only if migration is absent. If migration occurs one can use the generalization of the Yokota-Tanimoto expression given by Martin *et al.*[17,18]

$$I(t) = (\text{offset}) + I(0)\exp\left[-\frac{t}{\tau_r} - C_A Q t^{3/S} \times\left(\frac{1 + a_1 X + a_2 X^2}{1 + b_1 X}\right)^{(S-3)/(S-2)}\right] \tag{13}$$

where a_1, a_2, and b_1 are the Padé approximant coefficients, depending on the multipolar character of the interaction (see Ref. 18 for their values) and

$$X = D C_{DA}^{-2/S} t^{1-2/S} \tag{14}$$

where D is the diffusion coefficient that characterizes the energy transfer processes between ions. If D is zero (the migration between ions is negligible) the Inokuti-Hirayama formula is obtained.

The energy transfer probability between donors and acceptors can be expressed by

$$W_{i\text{-}i}(R_K) = \frac{C_{DA}^{(S)}}{R_K^S} \tag{15}$$

where R_K is the mean distance of separation between donor and acceptor. The R_K for which $W_{i\text{-}i}$ is equal to A_r is commonly called the "critical radius" (R_0).

The values of fitting parameters, in the limit of nonmigration processes only, are presented in the Table V.

A range of values of C_{DA} occurs in the literature for other ions.[18] The best fitting, the lowest χ^2, was obtained for the DD interaction in all three analyzed concentrations of samarium ions. The worst fit was the QQ interaction in all cases also.

When migration is taken into consideration, the fits of theoretically predicted curves to measured curves are better. The fitting parameters are presented in Table VI. It seems that the dominant mechanism, in crystals containing 5 at. % of Sm^{3+}, is DD. For crystals containing 10 at. % of Sm^{3+} all mechanisms (DD, DQ, QQ) are probable. In the case of material doped with 25 at. % the main interaction is DD but QQ should be also taking into consideration. The literature about

TABLE V. The kinetic microparameters C_{DA} related to the cross relaxation and R_0 calculated in the frame of Inokuti-Hirayama model (Ref. 16) for Sm^{3+} $K_5Li_2LaF_{10}$:Sm crystals.

Concentration (at. %) (ions/m^3)	S	R_0 (m^{-10})	C_{DA} (m^S/s)	χ^2
5	6	7.517	2.368×10^{-53}	0.0219
1.731×10^{26}	8	7.335	1.100×10^{-71}	0.0428
	10	7.177	4.761×10^{-90}	0.0650
10	6	7.968	3.360×10^{-53}	0.0468
3.463×10^{26}	8	7.357	1.127×10^{-71}	0.1096
	10	7.554	7.946×10^{-90}	0.2290
25	6	6.856	1.363×10^{-53}	0.1559
8.657×10^{26}	8	6.834	6.247×10^{-72}	0.5015
	10	6.705	2.413×10^{-90}	0.7804

Sm^{3+} luminescence properties is modest—Sm^{3+} is the least investigated lanthanide ion, except Pm^{3+}. It makes it difficult to compare the data presented here to those published for other systems. However, some research has been done. In particular, Zhang *et al.*[34] found, in samarium-doped borate glass, that the dominant interaction, in the cross-relaxation process, is the DD. On the other hand, Malinowski *et al.* discovered the DQ process in a KYP_4O_{12}:Sm^{3+} crystal[35] while Lavín *et al.* affirmed that the QQ interaction for the cross relaxation of the $^4G_{5/2}$ multiplet in fluoroborate glass can be determined as the dominant mechanism.[32] Unfortunately, Lavín *et al.* did not present the values of the kinetic microparameters C_{DA} and D, which may be useful in comparison. In their work the authors obtained a better fit of the theoretical curve for the Inokuti-Hirayama model than for the generalized Yakota-Tanimoto one. It seems strange, because addition of more parameters in the theoretical curve describing diffusion should make for better agreement. The same kind of interaction (QQ) was found by Mahato *et al.*

TABLE VI. The generalized Yakota-Tanimoto kinetic microparameters C_{DA} related to the cross relaxation and D related to the energy migration [Martin *et al.* (Ref. 18)].

Concentration (at. %) (ions/m^3)	S	C_{DA} (m^S/s)	D (m^2/s)	χ^2
5	6	1.680×10^{-53}	1.553×10^{-17}	0.0184
1.731×10^{26}	8	5.900×10^{-72}	2.497×10^{-17}	0.0209
	10	5.687×10^{-94}	2.922×10^{-16}	0.0559
10	6	2.120×10^{-53}	4.153×10^{-17}	0.0277
3.463×10^{26}	8	6.840×10^{-72}	5.259×10^{-17}	0.0340
	10	1.895×10^{-90}	1.023×10^{-16}	0.0391
25	6	4.190×10^{-54}	8.448×10^{-17}	0.0378
8.657×10^{26}	8	3.818×10^{-74}	2.071×10^{-16}	0.0703
	10	5.226×10^{-92}	1.023×10^{-16}	0.0476

for Sm^{3+}-doped oxyfluoroborate glass.[31] They obtained R_0 =9.0 Å, a value slightly bigger than in $K_5Li_2LaF_{10}$:Sm^{3+} (see Table V).

IV. CONCLUSIONS

This work reports basic spectroscopic investigations of $K_5Li_2La_{1-x}Sm_xF_{10}$, belonging to the family of uncommon stoichiometric luminescent compounds $K_5Li_2LnF_{10}$, where Ln denotes Ce, Nd, Pr, Sm, Eu, and Gd. It was found that in these crystals, the concentration quenching of luminescence is unusually weak, with some exceptions: the $^1D_2$ level of Pr^{3+} and the $^5D_3$ level of Eu^{3+}.[3,21] For small concentrations of the mentioned activators, the lifetimes of f^n excited states in $K_5Li_2LnF_{10}$, reach the longest values in all known lanthanide compounds.[21] In the case of the properties described here of the $^4G_{5/2}$ multiplet of Sm^{3+}, the lifetime attains 7600 and 80 μs for 1 and 100 at. % of Sm^{3+}, respectively, and is independent of temperature because cross-relaxation processes appear to be resonant. In the cross-relaxation processes the levels $^4G_{5/2}$, $^6F_{11/2}$, $^6H_{5/2}$, and $^6F_{5/2}$ take part. If the diffusion of energy is taken into consideration, higher kinds than, the dipole-dipole interaction of multipolar interaction should be taken into consideration, although for the basic Inokuti-Hirayama model, the dominant mechanism of cross-relaxation processes seems to be the dipole-dipole interaction. In all investigated $K_5Li_2La_{x-1}Sm_xF_{10}$ crystals, the hypersensitive transition is found to be weak, as observed in $K_5Li_2NdF_{10}$ and $K_5Li_2EuF_{10}$. This fact is unclear at this moment because of the very low symmetry of the local lanthanide ion environment, C_s. We plan a systematic investigation of the intensities of hypersensitive transitions in $K_5Li_2LnF_{10}$ systems, which seem to challenge theoretical models.

ACKNOWLEDGMENTS

The authors are grateful to Toyo Tanso Co., Ltd., Osaka, Japan for providing high-quality IG-110 purified graphite and to Dr. M. Wołcyrz for crystal structure measurements.

*Corresponding author. Fax: +48 71 344 1029. Email address: solarz@int.pan.wroc.pl

[1] A. Lempicki and B. C. McCollum, J. Lumin. **20**, 291 (1979).
[2] G. Dominiak-Dzik, S. Gołąb, M. Bałuka, A. Pietraszko, and K. Hermanowicz, J. Phys.: Condens. Matter **11**, 5245 (1999).
[3] P. Solarz and W. Ryba-Romanowski, J. Phys. Chem. Solids **64**, 1289 (2003).
[4] I. Sokólska, S. Gołąb, M. Bałuka, and W. Ryba-Romanowski, J. Lumin. **91**, 79 (2000).
[5] H. Danielmeyer and H. P. Weber, IEEE J. Quantum Electron. **8**, 805 (1972).
[6] H. G. Danielmeyer, Advances in Solid State Physics, edited by H. J. Quesser (Pergamon/Vieweg, Braunschweig, 1975), Vol. XV, p. 253.
[7] H. Y.-P. Hong, Acta Crystallogr., Sect. B: Struct. Crystallogr. Cryst. Chem. **30**, 468 (1974).
[8] H. P. Weber, T. C. Damen, H. G. Danielmeyer, and B. C. Tofield, Appl. Phys. Lett. **22**, 534 (1973).
[9] A. A. Kaminskii, S. E. Sarkisov, J. Bohm, P. Reiche, D. Schultze, and R. Uecker, Phys. Status Solidi A **43**, 71 (1977).
[10] W. Ryba-Romanowski and P. Solarz, Chem. Phys. Lett. **377**, 27 (2003).
[11] A. Ellens, H. Andres, M. L. H. ter Heerdt, R. T. Wegh, A. Meijerink, and G. Blasse, J. Lumin. **66–67**, 240 (1995).
[12] A. Ellens, H. Andres, A. Meijerink, and G. Blasse, Phys. Rev. B **55**, 173 (1997).
[13] A. Ellens, H. Andres, A. Meijerink, and G. Blasse, Phys. Rev. B **55**, 180 (1997).
[14] B. R. Judd, Phys. Rev. **127**, 750 (1962).
[15] G. S. Ofelt, J. Chem. Phys. **37**, 511 (1962).
[16] M. Inokuti and F. Hirayama, J. Chem. Phys. **43**, 1978 (1965).
[17] M. Yokota and O. Tanimoto, J. Phys. Soc. Jpn. **22**, 779 (1967).
[18] I. R. Martín, V. D. Rodríguez, U. R. Rodríguez-Mendoza, V. Lavín, E. Montoya, and D. Jaque, J. Chem. Phys. **111**, 1191 (1999).
[19] H. Y.-P. Hong, and B. C. McCollum, MRS Bull. **14**, 137 (1978).
[20] P. Solarz, I. Sokólska, and W. Ryba-Romanowski, J. Mol. Struct. **614**, 325 (2002).
[21] P. Solarz, Ph.D. thesis, Institute of Low Temperature and Structure Research, Polish Academy of Sciences, Wrocław, Poland, 2004.
[22] C. K. Jørgensen and B. R. Judd, Mol. Phys. **8**, 281 (1964).
[23] D. E. Henri, R. L. Fellows, and G. R. Choppin, Coord. Chem. Rev. **18**, 199 (1976).
[24] S. F. Mason, R. D. Peacock, and B. Steward, Chem. Phys. Lett. **29**, 149 (1974).
[25] S. F. Mason, R. D. Peacock, and B. Steward, Mol. Phys. **30**, 1829 (1975).
[26] A. Lempicki, B. C. McCollum, and S. R. Chinn, IEEE J. Quantum Electron. **15**, 896 (1979).
[27] C. K. Jayasankar and E. Rukmini, Opt. Mater. **8**, 193 (1997).
[28] S. Duffy, J.-P. R. Wells, H. G. Gallagher, and T. P. J. Han, J. Cryst. Growth **203**, 405 (1999).
[29] B. R. Judd, Phys. Scr. **21**, 543 (1980).
[30] J.-P. R. Wells, A. Sugiyama, Th. P. J. Han, and H. G. Gallagher, J. Lumin. **87–89**, 1029 (2000).
[31] K. K. Mahato, D. K. Rai, and S. B. Rai, Solid State Commun. **108**, 671 (1998).
[32] V. Lavín, I. R. Martin, C. K. Jayasankar, and Th. Tröster, Phys. Rev. B **66**, 064207 (2002).
[33] A. A. Kaminskii, I. M. Silvestrova, S. E. Sarkisov, and G. A. Denisenko, Phys. Status Solidi A **80**, 607 (1983).
[34] Z. Zhang, X. Jiang, Z. Li, P. Wu, and S. Xu, J. Lumin. **40–41**, 657 (1988).
[35] M. Malinowski, B. Jacquier, G. Boulon, and W. Wolińksi, J. Lumin. **39**, 301 (1988).